Research Article
Turkish Journal of Maritime and Marine Sciences
DOI: 10.52998/trjmms.1516839
Volume: 10 Special Issue: 1 (2024) 19-30

Performance evaluation of pre-equalized UVLC links over outdated lognormal turbulence channels

Pre-eşitlenmiş UVLC bağlantılarının eski lognormal türbülans kanalları üzerindeki performans değerlendirmesi

Türk Denizcilik ve Deniz Bilimleri Dergisi
Cilt: 10 Özel Sayı: 1 (2024) 19-30

Mohammed ELAMASSIE[1,*]
[1]*Department of Electrical and Electronics Engineering, Ozyegin University, Istanbul, Turkey.*

ABSTRACT

Underwater visible light communication (UVLC) is important for various underwater applications, including diver-to-diver information sharing, oil field exploration, port security, underwater surveillance systems, and environmental monitoring. However, it should be remembered that UVLC links are strongly affected by underwater optical turbulence (UOT). This may necessitate frequent adjustments in transmit power based on current channel state information (CSI) to mitigate fading effects. In some applications, such as diver-to-diver links, the quasi-static variations in the channel coefficient between transmission frames—attributable to the semi-fixed positions of the transmitting and/or receiving nodes—lead to practical implementations of the transmit power selection that may rely on outdated CSI. In this paper, we investigate the degradation in error rate performance caused by the use of outdated channel information in setting transmit power. Especially, we derive a closed-form expression for the bit error rate (BER) for a pre-equalized UVLC link over outdated lognormal turbulence channels. We verify the derived expression using Monte Carlo simulations.

Keywords: Underwater visible light communication, optical turbulence, diver-to-diver communication, outdated lognormal turbulence channels.

Article Info
Received: 16 July 2024
Revised: 02 September 2024
Accepted: 08 September 2024

* (corresponding author)
E-mail: mohammed.elamassie@ozyegin.edu.tr

To cite this article: Elamassie, M. (2024). Performance evaluation of pre-equalized UVLC links over outdated lognormal turbulence channels. *Turkish Journal of Maritime and Marine Sciences*, 10 (Special Issue: 1): 19-30. doi: 10.52998/trjmms.1516839.

ÖZET

Su altı görünür ışık iletişimi (UVLC), dalgıçtan dalgıca bilgi paylaşımı, petrol sahası keşfi, liman güvenliği, su altı gözetim sistemleri ve çevresel izleme gibi çeşitli su altı uygulamaları için önemlidir. Ancak, UVLC bağlantılarının su altı optik türbülansından (UOT) büyük ölçüde etkilendiği unutulmamalıdır. Bu durum, solma etkilerini azaltmak için mevcut kanal durumu bilgisine (CSI) dayalı olarak iletim gücünde sık sık ayarlamalar yapılmasını gerektirebilir. Dalgıçtan dalgıca bağlantılar gibi bazı uygulamalarda, iletim ve/veya alıcı düğümlerin yarı sabit pozisyonlarından kaynaklanan iletim çerçeveleri arasındaki kanal katsayısındaki yarı statik değişiklikler, iletim gücü seçiminin eski kanal verilerine dayanmasına yol açabilir. Bu çalışmada, iletim gücünün ayarlanmasında eski kanal bilgilerinin kullanılmasının hata oranı performansındaki bozulmayı araştırıyoruz. Özellikle, eski lognormal türbülans kanalları üzerinden önceden eşitlenmiş bir UVLC bağlantısı için bit hata oranı (BER) için kapalı formda bir ifade türetiyoruz. Türettiğimiz ifadeyi Monte Carlo simülasyonları kullanarak doğruluyoruz.

Anahtar sözcükler: Sualtı görünür ışık iletişimi, optik türbülans, dalgıçtan dalgıca iletişim, eski lognormal türbülans kanalları.

1. INTRODUCTION

The requirement for underwater communication systems is increasing due to the growing range of human activities underwater, such as underwater scientific data collection, environmental monitoring, oil field exploration, maritime archeology, port security and tactical surveillance (Elamassie *et al.*, 2023; Gussen *et al.*, 2016). Table I summarizes the potential uses, benefits, and limitations of visible light communications (VLC) in various underwater applications. It is important to note that prior to discussing wireless technologies, one should recognize that wire-line systems especially fiber-optic may offer real-time communication solutions underwater and remain a widely accepted and effective solution in some situations. However, wire-line systems are less adaptable and have several shortcomings in their operation, which make them not fully applicable. These limitations necessitate the need for underwater wireless technologies (Elamassie *et. al*., 2024).

Radio frequency (RF), acoustic, and optical are the three main underwater wireless technologies. The choice of which technology to use underwater depends on the mission requirements and applications. Minimum delay is offered by optical technology due to its high propagation speed. Moreover, optical has high security levels considering it mainly uses line-of-sight (LoS) configurations. These characteristics have made optical technology ideal for real-time, high-data-rate short-distance applications such as underwater imaging and video transmission amongst others. As a result, research into underwater VLC (UVLC) has been intensifying with topics ranging from channel modeling, to controlling propagation channel media, to physical layer and application layer (Gussen *et al.*, 2016; Zeng *et al.*, 2017; Saeed *et al.*, 2019; Ata *et al.*, 2023; Yildiz *et al.*, 2022; Weng *et al.*, 2019; Jiang *et al.*, 2020; Mahmoodi and Uysal, 2022; Wang *et al.*, 2023; Shi *et al.*, 2023; Qian *et al.*, 2023; Zhu *et al.*, 2023; Memon *et al.*, 2023; Hu *et al.*, 2023; Lu *et al.*, 2023; Salam *et al.*, 2023; Wei *et al.*, 2023; Celik *et al.*, 2023; Alqurashi *et al.*, 2023; Tang *et al.*, 2023; Ge and Zhu, 2023; Jiawei *et al.*, 2023; Agarwal and Singh, 2023, Elamassie *et al.*, 2023).

While underwater optical transmission could support high data rates, it is significantly affected by underwater optical turbulence (UOT). Random signal intensity fluctuations caused by fluctuations in refractive index due to salinity and temperature fluctuations within marine environment known as UOT. Bernotas and Nelson, (2015); Oubei *et al.*, (2017); Vali *et al.,* (2018); Jamali *et al.,* (2016), Jamali *et al.,* (2018) have studied the statistical distribution of this underwater fading and it has been found that measurement results generally fit both Lognormal (LN) and Gamma-Gamma (GG)

probability density functions which correspond to weak turbulence (WT) and moderate/strong turbulence (MT/ST) conditions respectively. Different viable methods have been presented in the open literature to mitigate the effect of UOT. The widely known one among these is the multiple input multi-output (MIMO) system, which has proved successful in combating fading while exploiting spatial diversity (M. V. Jamali. Nabavi, and J. A. Salehi, 2018). Transmit laser selection (TLS) is another method that effectively eliminates fading with manageable complexity and achieves full diversity gain benefits (Elamassie *et al.*, 2019). In addition, multi-hop serial relaying enhances link distances, energy efficiency improvement as well as cooperative diversity gains (Jamali *et al.*, 2017). It should be however considering that underwater communication possesses unique characteristics, particularly concerning energy availability. Therefore, in good channel conditions, conserving energy by transmitting at low power is needed. Conversely, in poor channel conditions such as weak channel fading coefficient, higher power levels may be used, resulting in more energy consumption in this case. Therefore, one of the possible solutions for mitigating fading coefficient is adaptive power transmission where the transmit power is selected based on the current channel state information (CSI). Most of the literature research works on adaptive optical communication.

Table 1. Potential Applications of UVLC.

Application	Explanation	Limitations
Oil Field Exploration	Data transmission between underwater exploration equipment.	The water in oil fields can be turbid, which might affect the range and reliability.
Port Security	Enhancing underwater surveillance systems with high-speed data rates.	The turbidity and particulate matter in port waters may limit the effective range.
Environmental Monitoring	Data transmission from sensors monitoring water quality and marine life.	In highly turbid waters, the effectiveness of VLC might be reduced.
Oceanographic Data Collection	Real-time data transmission from various oceanographic instruments.	Depth and water clarity could impact the effectiveness of VLC.
Submarine Communication	Facilitating short-range high-speed communication between submarines.	Limited range and line-of-sight requirements may pose challenges.
Autonomous Underwater Vehicles (AUVs)	Facilitating high-speed data transfer and coordination between AUVs.	Line-of-sight and water clarity issues might limit range and reliability.
Diver Communication Systems	Providing reliable communication for divers, especially in clear waters.	Limited range and the need for line-of-sight may be challenging in some environments.
Underwater Surveillance	Transmitting high-resolution images and video for surveillance.	Effectiveness may be reduced in turbid or particulate-laden waters.
Underwater Robotics	Controlling and receiving data from underwater robots.	Line-of-sight and range limitations may affect usability in complex underwater environments.
Marine Archaeology	Transmitting data and images from underwater archaeological sites.	Water clarity and the need for line-of-sight could pose challenges.
Aquaculture	Monitoring fish behavior and environmental conditions in fish farms.	Limited by water clarity and potential obstructions in fish farming setups.
Recreational Applications	Providing real-time information and enhance underwater tours.	Range and line-of-sight requirements could be a challenge in recreational settings.
Disaster Recovery and Search Operations	Real-time communication and data transmission in search and rescue operations.	Water turbidity and debris may impact the effectiveness of VLC.

systems (Gubergrits *et al.*, 2007; Safi *et al.*, 2019) were built upon the assumption that the CSI is not outdated. In other words, assuming quasi-static (slowly changing) channels, the changes of CSI for a block period of time are neglected. However, an adaptive system requires processing time for estimating CSI, feedback it to the transmitter, and adapting/tuning the transmit parameters. Considering that, in practice, CSI varies continuously (even if the change is slight), the adaptive transmission is based on outdated information. Moreover, the coherence time of the optical channel underwater is generally in the range of 10^{-5} to 10^{-2} sec (S. Tang *et al.*, 2013). Therefore, since the adaptation must be at a rate that is not less than the frequency of channel changes (Elamassie and Uysal, 2021), CSI should be estimated and fed back to the transmitter hundreds, if not thousands, of times per second. Otherwise, CSI is outdated.

When dealing with outdated CSI in certain underwater applications, such as diver-to-diver VLC links or autonomous underwater vehicles (UUV) to sensor nodes, it implies that the parameters for transmission and/or reception may be selected or optimized from channel coefficients that no longer accurately reflect current conditions. This discrepancy arises because these platforms are not perfectly stable. The mismatch between the outdated CSI and the actual CSI can result in suboptimal performance or even communication failure, as the parameters are chosen based on outdated CSI rather than the current one. This issue has previously been addressed in the context of airborne free space optical (FSO) links, where a model for outdated log-normal fading in relay-assisted airborne FSO communication systems was proposed in (Elamassie *et al.*, 2023). Authors have then discussed the utilization of amplification factor based on turbulence strength to ensure signal reception above a targeted threshold even if the channel is outdated.

In this paper, we examine how the selection of transmit power, based on outdated lognormal channel conditions, impacts the BER performance. Specifically, we derive a closed-form expression for the BER of pre-equalized UVLC links operating over outdated lognormal turbulence channels. We validated the derived expression through Monte Carlo simulations. Furthermore, we start the simulation by performing thorough numerical simulations that evaluate the accuracy of outdated lognormal turbulence channel models.

The remainder of the paper is arranged as follows. In Section 2, we present the considered UVLC system model and discuss the outdated lognormal channel. In Section 3, we derive a closed form expression for BER of the considered links over outdated lognormal turbulence channels. Numerical and simulation results are presented in Section 4. We conclude our paper in Section 5.

Notation: Let y be distributed as $\mathcal{LN}\left(\mu,\sigma^2\right)$, indicating y follows a lognormal distribution with mean μ and variance σ^2. Let x be distributed as $\mathcal{N}\left(\mu_n,\sigma_n^2\right)$, indicating x follows a normal distribution with mean μ_n and variance σ_n^2.

2. SYSTEM AND CHANNEL MODELS

As illustrated in Fig. 1, we consider a Diver to Diver UVLC link. The link distance is given by d. Transmit Diver (Denoted by S) is equipped with one laser source with electro-optical conversion factor of η and the receive Diver (Denoted by D) is equipped with one photodetector with opto-electrical conversion factor of r. We assume intensity-modulation direct-detection (IM/DD).

Let x represent the transmitted signal using M-ary unipolar pulse amplitude modulation (M-UPAM). We consider the fading channel coefficient I, which follows a lognormal distribution with variance σ^2 and mean μ, denoted as $I \sim \mathcal{LN}\left(\mu,\sigma^2\right)$. To guarantee that the average power remains unaffected by the channel fading coefficient, it is necessary to normalize the coefficient, implying $\mu = -0.5\sigma^2$. The received signal can be detected with an outdated version of the fading channel coefficient I_{out}. From a mathematical standpoint, the received signal can be expressed as

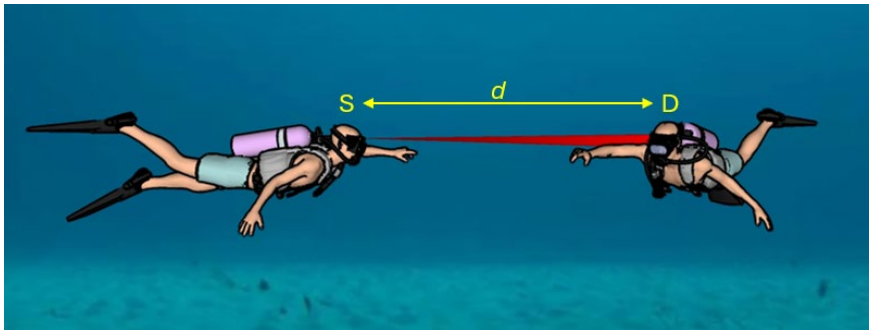

Figure 1. Diver to Diver UVLC Link.

$$y = \sqrt{P_{\text{te}}}\,\eta r h I_{\text{out}} x + w, \tag{1}$$

where h and w denote, respectively, channel deterministic attenuation term and additive white Gaussian noise (AWGN) term with zero mean, i.e., $w \sim \mathcal{N}\left(0, \sigma_n^2\right)$ with σ_n^2 denoting the noise variance. In (1), P_{te} represents the mean electrical transmission power, chosen to ensure that the signal is received with a required power level of P_{req} as

$$P_{\text{te}} = \left(1 / \eta^2 r^2 h^2 I^2\right) P_{\text{req}} \cdot \tag{2}$$

By substituting (2) into (1), the received signal can be expressed as

$$y = \sqrt{P_{\text{req}}}\left(\frac{I_{\text{out}}}{I}\right) x + w, \tag{3}$$

indicating that the signal will achieve exactly the necessary power reception only under the condition that the fading channel coefficient remains unchanged (i.e., $I_{\text{out}} = I$).

Feedback from the receiving node to the transmitting node is required for effective implementation of transmit power selection. In diver-to-diver links, UVLC has channel coefficient that may vary from frame to another due to divers being rather non-stationary. As previously denoted, I_{out} represents the outdated version of I and modeled as (Elamassie *et al.*, 2023, eq. (9))

$$I_{\text{out}} = \rho I + (1-\rho) e, \tag{4}$$

where ρ denotes the normalized correlation coefficient and e denotes the channel errors. The fading channel coefficient represents the instantaneous channel condition that varies over time. The 'current' coefficient refers to the present condition, while the 'outdated' one refers to a past coefficient. These coefficients, though from different times, are considered samples from the same underlying probability distribution function, assuming unchanged turbulence strength. This implies that the outdated version of the lognormal fading coefficient (i.e., I_{out}) follows the same lognormal distribution of I , i.e., $I_{\text{out}} \sim \mathcal{LN}\left(\mu, \sigma^2\right)$. To satisfy this, e follows also lognormal distribution with variance $\sigma_e^2 = \sigma^2\left[(1+\rho)/(1-\rho)\right]$ and mean $\mu_e = \mu$, i.e.,

$$e \sim LN\left(\mu, \frac{(1+\rho)}{(1-\rho)}\sigma^2\right), \quad \rho \neq 1 \cdot \tag{5}$$

3. DERIVATION OF BER

It can be noted that the power level of the signal received in equation (3) depends on both the fading coefficient (I) and its outdated version (I_{out}). I_{out} itself is a function of two independent random variables (i.e., I and e). If we define $z = \rho + (1-\rho) e I^{-1}$, we can write the received single as a function of single random variable as

$$y = \sqrt{P_{\text{req}}}\, z x + w, \tag{6}$$

Here, the received instantaneous SNR can simply

be defined as $\gamma_{\text{ins}} = \gamma z^2$ with γ denoting the fading free SNR and given as $\gamma = P_{\text{req}} / \sigma_n^2$. As a sanity check, when the channel is not outdated (i.e., $\rho = 1$), the signal will be detected with the required power (i.e., $y = \sqrt{P_{\text{req}}}x + w$).

For U-PAM, the conditional BER (i.e., conditioned on z) takes the form of

$$BER_c = F\,\text{erfc}\left(\sqrt{C\gamma}\, z\right), \tag{7}$$

where $F = (M-1)/\left(M\log_2(M)\right)$ and $C = 3/\left(2(M-1)(2M-1)\right)$. Taking an expectation of (7) with respect to z, we can obtain the average BER as

$$BER = F\int_{-\infty}^{\infty} \text{erfc}\left(\sqrt{C\gamma}\, z\right) f_z(z)\, dz\cdot \tag{8}$$

Performing the integration in (8) requires finding the PDF of $z = \rho + (1-\rho)eI^{-1}$. Recall that $I \sim \mathcal{LN}\left(\mu, \sigma^2\right)$ and $e \sim \mathcal{LN}\left(\mu_e, \sigma_e^2\right)$ are two Independent but Not Identically Distributed (i.n.i.d) lognormal random variables. If we utilize the fact that $\ln\left(x^{-1}\right) = -\ln(x)$, the PDF of I^{-1} can be simply written as

$$I^{-1} \sim LN\left(-\mu, \sigma^2\right)\cdot \tag{9}$$

The PDF of $I^{-1}e$, i.e., the PDF of the product of two i.n.i.d lognormal random variables, follows lognormal and is given by (Drew *et al.*, 2017, Chapter 6) where the overall mean and variance are simply found, respectively, as the summation of means and variances as

$$eI^{-1} \sim LN\left(0, \sigma_e^2 + \sigma^2\right)\cdot \tag{10}$$

The PDF of lognormal random variable multiplied by constant $(1-\rho)$ is obtained by shifting the mean by $\ln(1-\rho)$ (Romeo *et al.*, 2013). Therefore, the PDF of $(1-\rho)eI^{-1}$ is obtained as

$$(1-\rho)eI^{-1} \sim LN\left(\ln(1-\rho), \sigma_e^2 + \sigma^2\right)\cdot \tag{11}$$

The PDF of $z = \rho + (1-\rho)eI^{-1}, z \geq \rho$ can then be obtained by using density transformation (Solomon and Breckon, 2011, Eq. (3.11)) as

$$f_z(z) = \frac{1}{(z-\rho)\sqrt{2\pi\left(\sigma_e^2 + \sigma^2\right)}} \times \exp\left(-\frac{\left(\ln(z-\rho) - \left(\ln(1-\rho)\right)\right)^2}{2\left(\sigma_e^2 + \sigma^2\right)}\right). \tag{12}$$

If we replace (12) in (8), the average BER can be expressed as

$$BER = \frac{F}{\sqrt{2\pi\left(\sigma_e^2 + \sigma^2\right)}}\int_0^{\infty} \frac{\text{erfc}\left(\sqrt{C\gamma}\, z\right)}{(z-\rho)} \times \exp\left(-\frac{\left(\ln(z-\rho) - \left(\ln(1-\rho)\right)\right)^2}{2\left(\sigma_e^2 + \sigma^2\right)}\right) dz\cdot \tag{13}$$

If the integration variable in (13) is changed of $\xi = \left(\ln(z-\rho) - \left(\ln(1-\rho)\right)\right)\Big/\sqrt{2\left(\sigma_e^2 + \sigma^2\right)}$, (13) can be written as

$$BER = \frac{F}{\sqrt{\pi}}\int_{-\infty}^{\infty} \exp\left(-\xi^2\right) \times \text{erfc}\left(\sqrt{C\gamma}\left(\begin{matrix}(1-\rho)\exp\left[\sqrt{2\left(\sigma_e^2 + \sigma^2\right)}\xi\right] \\ +\rho\end{matrix}\right)\right) d\xi\cdot \tag{14}$$

Using the Gauss-Hermite rule, one can express (14) as a truncated sum (Abramowitz and Stegun,1972, Eq. (25.4.46)) as

$$BER \approx \frac{F}{\sqrt{\pi}}\sum_{i=1}^{l} w_{i,l} \times \text{erfc}\left(\sqrt{C\gamma}\left(\begin{matrix}(1-\rho)\exp\left[\sqrt{2\left(\sigma_e^2 + \sigma^2\right)}x_{i,l}\right] \\ +\rho\end{matrix}\right)\right), \tag{15}$$

where l is the approximation order, $x_{i,l}$, $i = 1,2,3,\cdots,l$ is the set of roots defined by

$H_l(x)=0$ with $H_l(x)$ denoting the physicists Hermite polynomial. In (15), $w_{i,l}$, $i=1,2,3,\cdots,l$ are the corresponding weights to $x_{i,l}$.

4. SIMULATION RESULTS

In this section, we first present simulation results validating the expressions for outdated lognormal channel in (4). We then investigate the effect of normalized correlation coefficient on error rate performance and validate our derived closed-form BER expression in (15) via Monte-Carlo simulation results. Unless stated otherwise, we assume modulation order of $M=4$ and fading free SNR in the range of $0\text{ dB}\le\gamma\le 30\text{ dB}$.

In the following, we first confirm that both of the channel fading coefficient (I) and its outdated version (I_{out}) have almost similar distributions for weak turbulence conditions of $\sigma^2<1$. We consider different values of log-amplitude variance of $\sigma^2=1\times10^{-3}$, $\sigma^2=1\times10^{-2}$, and $\sigma^2=1\times10^{-1}$. We further consider normalized correlation coefficients of $\rho=0$, $\rho=0.25$, $\rho=0.50$, $\rho=0.75$, and $\rho=1$.

In Fig. 2, we present the histogram of I_{out} along with the PDF of fading coefficient I. Outdated channel fading coefficients (I_{out}) are calculated through (4). Particularly, channel fading coefficients (I) in (4) are generated using lognormal distribution with mean μ and variance σ^2. Similarly, channel error coefficients (e) in (4) are generated using mean $\mu_e=\mu$ and variance $\sigma_e^2=(1+\rho)/(1-\rho)\sigma^2$ $\rho\neq1$, (see (5)).

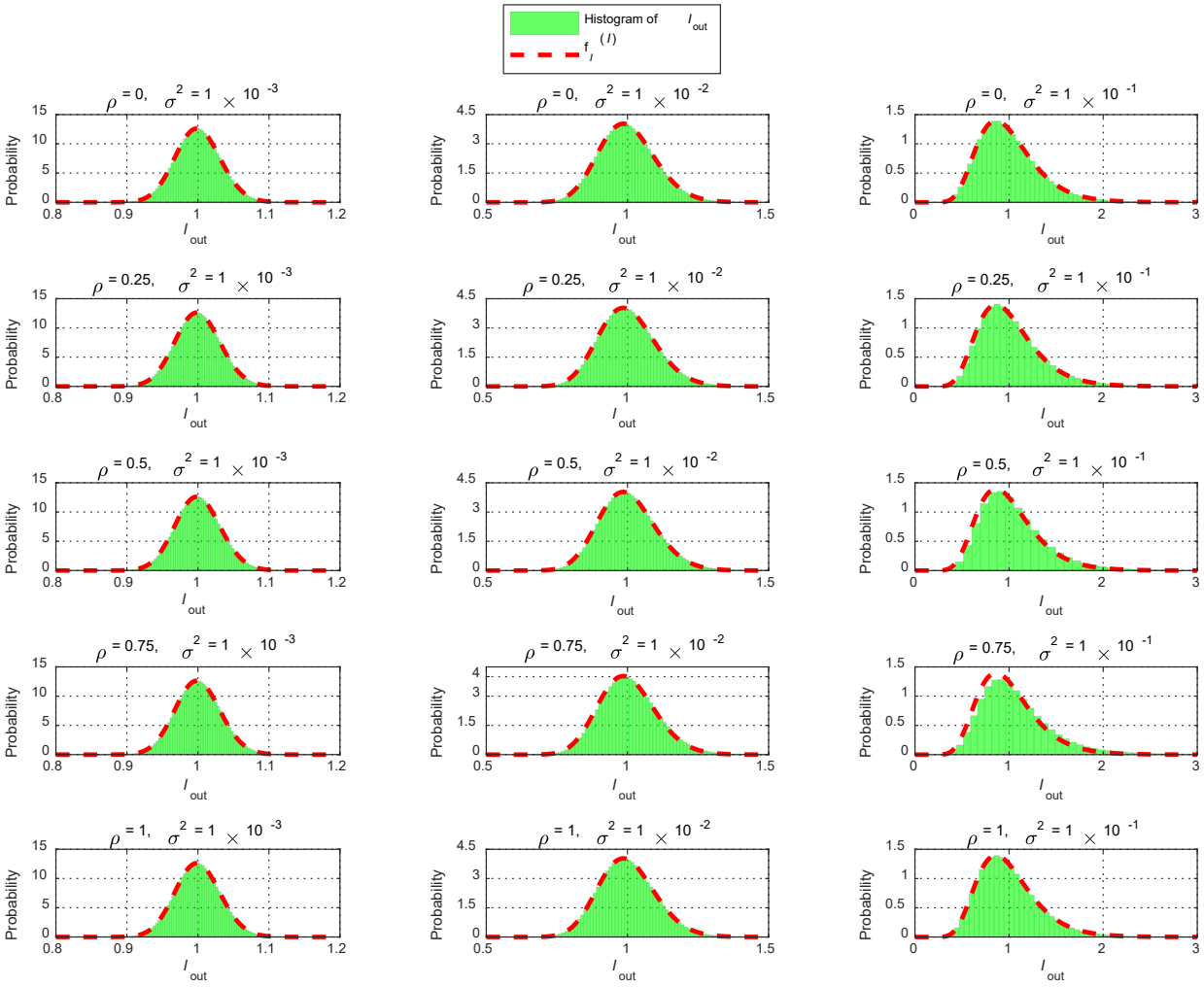

Figure 2. Statistical distribution of I_{out}.

It can be observed for $\sigma^2 < 0.1$ that the histogram of I_{out} coincides with the PDF of I, regardless of the value of normalized correlation coefficient (ρ). As σ^2 become larger, the histogram of I_{out} very slightly deviates from the PDF of I where the deviations depends on the normalized correlation coefficient (ρ).

In the following, we investigate the effect of normalized correlation coefficient on BER values considering log-amplitude variance of $\sigma^2 = 1\times10^{0}$, 1×10^{-1}, 1×10^{-2} and 1×10^{-3} in Figs. 3.a, 3.b, 3.c and 3.d, respectively. For the case of $\rho = 1$, theoretical BER in (7) is used after setting $z = 1$. Our results demonstrated that our derived BER expression in (15) provides a perfect match in all scenarios under consideration confirming the preciseness of our derivations.

On the other hand, while it is known that the outdated channel coefficient (I_{out}) may be larger or smaller than the known channel coefficient at the transmitter side (I), indicating that the instantaneous BER may be larger or smaller than the desired value at a certain SNR, it can be clearly observed from Figs. 3.a, 3.b, 3.c and 3.d that average BER for the case of outdated channel is worse where the smaller the correlation coefficient, the larger the average BER. In other words, higher SNR is needed to achieve the same targeted BER values as long as the normalized correlation coefficient becomes smaller. For example, the required SNR in order to achieve a BER of 10^{-6} assuming

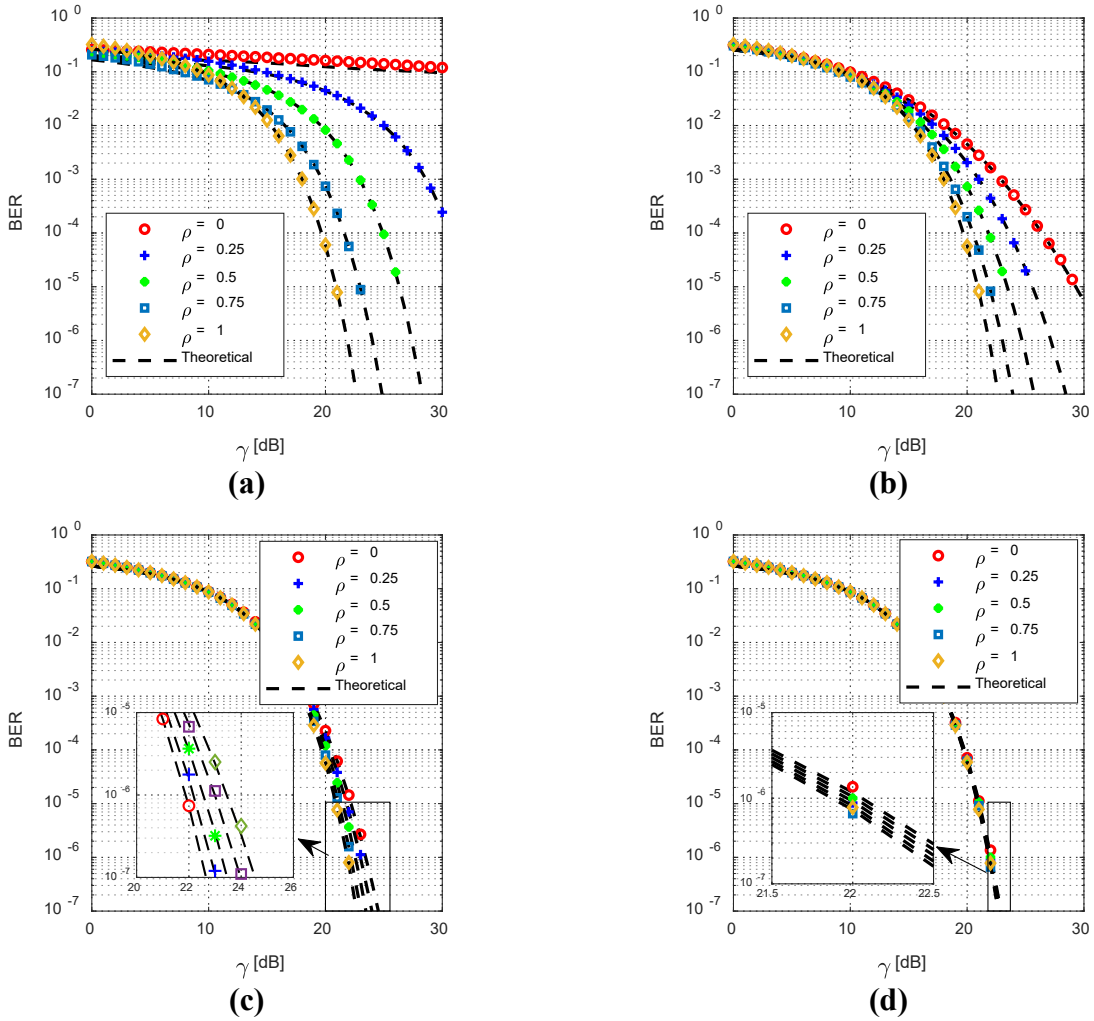

Figure 3. Effect of normalized correlation coefficient on BER: (a) $\sigma^2 = 1\times10^{0}$, (b) $\sigma^2 = 1\times10^{-1}$, (c) $\sigma^2 = 1\times10^{-2}$ and (d) $\sigma^2 = 1\times10^{-3}$.

$\sigma^2 = 1\times10^{-1}$ and normalized correlation coefficient of $\rho = 1$ is $\gamma = 21.88$ dB. This climbs for normalized correlation coefficient of $\rho = 0.75$, 0.5, and 0.25 assuming the same log amplitude variance of $\sigma^2 = 1\times10^{-1}$ to 23.02 dB, 24.67 dB, 27.16 dB. Indicating additional SNR of 1.14 dB, 2.79 dB, and 5.28 dB. It can also be observed that the targeted BER of 10^{-6} cannot be satisfied within the available SNR for zero normalized correlation coefficient, i.e., $\rho = 0.0$. Additionally, the change in average BER is more pronounced for larger turbulence strength (i.e., larger σ^2). For example, the required SNR in order to achieve a BER of 10^{-6} is $\gamma = 21.88$ dB assuming a normalized correlation coefficient of $\rho = 1$. This climbs for $\rho = 0.75$ to 23.75 dB, 23.02 dB, 22.18 dB, and 21.92 assuming, respectively, log-amplitude variance of $\sigma^2 = 1\times10^{-0}$, 1×10^{-1}, 1×10^{-2} and 1×10^{-3}. Indicating additional SNR of 1.87 dB, 1.14 dB, 0.30 dB, 0.04 dB, respectively.

5. CONCLUSIONS

We considered weak UOT that is modeled by lognormal fading and studied how transmit power selection based on outdated lognormal channel affects the BER performance. In particular, we derived a closed-form BER expression for pre-equalized UVLC links over outdated lognormal turbulence channels and validated our findings through Monte Carlo simulations. Our results demonstrated that the average BER deteriorates when channel information is outdated. The level of deterioration depends on the correlation

coefficient (ρ) and the turbulence strength (σ^2). Particularly, as the correlation coefficient decreases, the average BER increases, especially for higher turbulence strengths.

CONFLICT OF INTERESTS

The author declares that for this article he has no actual, potential, or perceived conflict of interests.

ETHICS COMMITTEE PERMISSION

No ethics committee permissions are required for this study.

FUNDING

No funding was received from institutions or agencies for the execution of this research.

ORCID IDs:

Mohammed ELAMASSIE:
https://orcid.org/0000-0001-9416-3860

6. REFERENCES

Abramowitz, M., Stegun, I.A. (1972). *Handbook of Mathematical Functions*. US Govt. printing, USA, 10 edition.

Agarwal, A., Singh, K. (2023). Energy-efficient UOWC-RF systems with SLIPT. *Transactions on Emerging Telecommunications Technologies*, e4889.

Alqurashi, F.S., Trichili, A., Saeed, N., Ooi, B.S., Alouini, M.S. (2023). Maritime communications: A survey on enabling technologies, opportunities, and challenges. *IEEE Internet Things Journal*, 10(4): 3525–3547.

Ata, Y., Abumarshoud, H., Bariah, L., Muhaidat, S., Imran, M.A. (2023). Intelligent reflecting surfaces for underwater visible light communications. *IEEE Photonics Journal*, 15(1): 1–10.

Bernotas, M., Nelson, C. (2015). Probability density function analysis for optimization of underwater optical communications systems. In OCEANS 2015 - MTS/IEEE Washington, pp.1–8.

Celik, A., Romdhane, I., Kaddoum, G., Eltawil, A.M. (2023). A top-down survey on optical wireless communications for the internet of things. IEEE *Communication Surveys & Tutorials*, 25(1): 1–45.

Drew, J.H., Evans, D.L., Glen, A.G., Leemis, L.M. (2017). *Computational Probability: Algorithms and Applications in the Mathematical Sciences*. Springer Publishing Company, 2nd edition.

Elamassie, M., Al-Nahhal, M., Kizilirmak, R.C., Uysal, M. (2019). Transmit laser selection for underwater visible light communication systems. In 2019 IEEE 30th Annual International Symposium on Personal, Indoor and Mobile Radio Communications (PIMRC), pp. 1–6.

Elamassie, M., Al-Shaikhi, A.A., Sait, S.M., Uysal, M. (2023). Multihop airborne FSO systems with relay selection over outdated log-normal turbulence channels. *IEEE Transactions on Vehicular Technology*, 1–13.

Elamassie, M., Geldard, C., Popoola, W. (2024). Underwater Visible Light Communication (UVLC). In: Kawanishi, T. (eds) Handbook of Radio and Optical Networks Convergence. Springer, Singapore. doi: 10.1007/978-981-33-4999-5_62-1

Elamassie, M., Uysal, M. (2021). Feedback-free adaptive modulation selection algorithm for FSO systems. *IEEE Wireless Communication Letters*, 10(9): 1964–1968.

Elamassie, M., Miramirkhani, F., Uysal, M. (2019). Performance Characterization of Underwater Visible Light Communication. *IEEE Transactions on Communications*, 67(1): 543-552.

Ge, X., Zhu, X. (2023). Mathematical modeling of underwater signal anomaly perception based on multi-sensor data fusion. *Journal of Computational Methods in Sciences and Engineering*, 23(1): 23–36.

Gubergrits, M., Goot, R.E., Mahlab, U., Arnon, S. (2007). Adaptive power control for satellite to ground laser communication. *International Journal of Satellite Communications and Networking*, 25(4): 349–362.

Gussen, C.M.G., Diniz, P.S.R., Campos, M.L.R., Martins, W.A., Gois, J.N. (2016). A survey of underwater wireless communication technologies. *Journal of Communication and Information Systems*, 31(1): 242–255.

Hu, Q., Huang, N., Gong, C. (2023). Superposition modulation for physical layer security in water-to-air visible light communication systems. *Journal of Lightwave Technology*, 41(10): 2976–2990.

Jamali, M.V., Chizari, A., Salehi, J.A. (2017). Performance analysis of multi-hop underwater wireless optical communication systems. *IEEE Photonics Technology Letters*, 29(5): 462–465.

Jamali, M.V., Khorramshahi, P., Tashakori, A., Chizari, A., Shahsavari, S., Abdollah Ramezani, S., Fazelian, M., Bahrani, S., Salehi, J.A. (2016). Statistical distribution of intensity fluctuations for underwater wireless optical channels in the presence of air bubbles. In Iran Workshop on Communication and Information Theory (IWCIT), pp. 1–6.

Jamali, M.V., Mirani, A., Parsay, A., Abolhassani, B., Nabavi, P., Chizari, A., Khorramshahi, P., Abdollahramezani, S., Salehi, J.A. (2018). Statistical studies of fading in underwater wireless optical channels in the presence of air bubble, temperature, and salinity random variations. *IEEE Transactions on Communications*, 66(10): 4706–4723.

Jamali, M.V., Nabavi, P., Salehi, J.A. (2018). MIMO underwater visible light communications: Comprehensive channel study, performance analysis, and multiple-symbol detection. *IEEE Transactions on Vehicular Technology*, 67(9): 8223–8237.

Jiang, H., Qiu, H., He, N., Popoola, W., Ahmad, Z., Rajbhandari, S. (2020). Performance of spatial diversity DCO-OFDM in a weak turbulence underwater visible light communication channel. *Journal of Lightwave Technology*, 38(8): 2271–2277.

Jiawei, H., Xiaoqian, L., Xinke, T., Yuhan, D. (2023). Trajectory planning of UUV-assisted UWOC systems based on DQN. *Telecommunications Science* 39(5).

Lu, H.H., Li, C.Y., Tsai, W.S., Chen, Y.X., Fan, W.C., Lin, Y.S., Peng, Y.E., Tang, Y.S. (2023). 5G-based triple-wavelength VLLC-UWLT and laboratory-lighting convergent systems. *Journal of Lightwave Technology*, 41(8): 2351–2360.

Mahmoodi, K.A., Uysal, M. (2022). Energy aware trajectory optimization of solar powered AUVs for optical underwater sensor networks. *IEEE Transactions on Communications*, 70(12): 8258–8269.

Memon, M.H., Yu, H., Jia, H., Fang, S., Wang, D., Zhang, H., Xiao, S., Kang, Y., Ding, Y., Gong, C., Sun, H. (2023). Quantum dots integrated deep ultraviolet micro-LED array toward solar-blind and visible light dual-band optical communication. *IEEE Electron Device Letters*, 44(3): 472–475.

Oubei, H.M., Zedini, E., ElAfandy, R.T., Kammoun, A., Abdallah, M., Ng, T.K., Hamdi, M., Alouini, M. S., Ooi, B.S. (2017). Simple statistical channel model for weak temperature induced turbulence in underwater wireless optical communication systems. *Optics Letters*, 42(13): 2455–2458.

Qian, Y., Chen, C., Du, P., Liu, M. (2023). Hybrid space division multiple access and quasi-orthogonal multiple access for multi-user underwater visible light communication. *IEEE Photonics Journal*, 15(4): 1–7.

Romeo, M., Da Costa, V., Bardou, F. (2003). Broad distribution effects in sums of lognormal random variables. *The European Physical Journal B - Condensed Matter and Complex Systems*, 32(4): 513–525.

Saeed, N., Celik, A., Al-Naffouri, T.Y., Alouini, M.S. (2019). Underwater optical wireless communications, networking, and localization: A survey. *Ad Hoc Networks*, 94: 101935.

Safi, H., Sharifi, A.A., Dabiri, M.T., Ansari, I.S., Cheng, J. (2019). Adaptive channel coding and power control for practical FSO communication systems under channel estimation error. *IEEE Transactions on Vehicular Technology*, 68(8): 7566–7577.

Salam, R., Srivastava, A., Bohara, V.A., Ashok, A. (2023). An optical intelligent reflecting surface-assisted underwater wireless communication system. *IEEE Open Journal of the Communications Society*, 4: 1774–1786.

Shi, J., Niu, W., Li, Z., Shen, C., Zhang, J., Yu, S., Chi, N. (2023). Optimal adaptive waveform design utilizing an end-to-end learning-based pre-equalization neural network in an UVLC system. *Journal of Lightwave Technology*, 41(6): 1626–1636.

Solomon, C., Breckon, T. (2011). *Fundamentals of Digital Image Processing: A practical approach with examples in Matlab*. John Wiley & Sons, New York, NY, USA, 1 edition.

Tang, S., Zhang, X., Dong, Y. (2013). Temporal statistics of irradiance in moving turbulent ocean. In MTS/IEEE OCEANS - Bergen, pp. 1–4.

Tang, Y., Ding, X., Li, Z., Shao, C., Huang, Z., Liang, S. (2023). Crosstalk-free MIMO VLC using two orthogonal polarizations multiplexed large FoV fluorescent antennas. *IEEE Photonics Technology Letters*, 35(23): 1271–1274.

Vali, Z., Gholami, A., Ghassemlooy, Z., Omoomi, M., Michelson, D.G., (2018). Experimental study of the turbulence effect on underwater optical wireless communications. *Applied Optics*, 57(28): 8314–8319.

Wang, K., Song, T., Wang, Y., Fang, C., He, J., Nirmalathas, A., Lim, C., Wong, E., Kandeepan, S. (2023). Evolution of short-range optical wireless communications. *Journal of Lightwave Technology*, 41(4): 1019–1040.

Wei, Z., Wei, Z., Fang, J., Pan, J., Wang, L., Dong, Y. (2023). Impulse response modeling and dynamic analysis for SIMO UOWC systems enhanced by RIS equipped UUV. *IEEE Transactions on Vehicular Technology*, pp. 1–14.

Weng, Y., Guo, Y., Alkhazragi, O., Ng, T.K., Guo, J.H., Ooi, B.S. (2019). Impact of turbulent-flow-induced scintillation on deep-ocean wireless optical communication. *Journal of Lightwave Technology*, 37(19): 5083–5090.

Yildiz, S., Baglica, I., Kebapci, B., Elamassie, M., Uysal, M. (2022). Reflector-aided underwater optical channel modeling. *Optics Letters*, 47(20): 5321–5324.

Zeng, Z., Fu, S., Zhang, H., Dong, Y., Cheng, J. (2017). A survey of underwater optical wireless communications. *IEEE Communication Surveys Tutorials*, 19(1): 204–238.

Zhu, Z., Lei, L., Lin, T., Li, L., Lin, Z., Jiang, H., Li, G., Wang, W. (2023). Embedded electrode micro-LEDs with high modulation bandwidth for visible light communication. *IEEE Transactions on Electron Devices*, 70(2): 588–593.